International Journal of Engineering & Technology, 7 (4.35) (2018) 551-558

International Journal of Engineering & Technology

Website: www.sciencepubco.com/index.php/IJET

Research paper



Comparative Prediction of Red Alga Biosorbent Performance in Dye Removal using Multivariate Models of Response Surface Methodology (RSM) and Artificial Neural Network (ANN)

Nadiah Mokhtar[1*], Edriyana A.Aziz [2], Azmi Aris [3] ,W.FW.Ishak[4], Anwar P.P. Abdul Majeed[5], Syazwan N.Moni[6], Siti Kamariah Md Sa'at[7]

[1,2,6]*Faculty of Civil Engineering and Earth Resources, Universiti Malaysia Pahang, Lebuhraya Tun Razak, 26300 Gambang, Kuantan, Pahang, Malaysia.*

[3]*Centre for Environmental Sustainability & Water Security (IPASA), Research Institute for Sustainable Environment, Block C07, Level 2, Universiti Teknologi Malaysia, 81310 UTM Johor Bahru, Johor, Malaysia.*

[4]*Faculty of Bioengineering and Technology, Universiti Malaysia Kelantan, Jeli Campus, Locked Bag No.100, 17600 Jeli, Kelantan, Malaysia.*

[5]*Innovative Manufacturing, Mechatronics and Sports (iMAMS) Laboratory, Faculty of Manufacturing Engineering, Universiti Malaysia Pahang, 26600, Pekan, Pahang, Malaysia*

[7]*School of Bioprocess Engineering, Jejawi 3School Complex, Universiti Malaysia Perlis, 02600 Arau, Perlis, Malaysia*

**Corresponding author E-mail: nadiah@ump.edu.my*

Abstract

Red algae species, *Euchema Spinosum* (*ES*) in Malaysia possesses excellent biosorbent properties in removing dyes from aqueous solutions. In the present study, the experimental design for the biosorption process was carried out via response surface methodology (RSM-CCD). A total of 20 runs were carried out to generate a quadratic model and further analysed for optimisation. Prior to the evaluation, the characterisation study of the *ES* was performed. It was observed that the maximum uptake capacity of 399 mg/g (>95%) is obtained at equilibrium time of 60 min, pH solution of 6.9-7.1, dosage of 0.72 g/L and initial dye concentration of 300 g/L through statistical optimisation (CCD-RSM) based on the desirability function. It is demonstrated in the present study that the ANN model (R^2=0.9994, adj-R^2=0.9916, MSE=0.19, RMSE=0.4391, MAPE=0.087 and AARE=0.001) is able to provide a slightly better prediction in comparison to the RSM model (R^2= 0.9992, adj-R^2= 0.9841, MSE=1.95, RMSE=1.395, MAPE=0.08 and AARE=0.001). Moreover, the SEM-EDX analysis indicates the development of a considerable number of pore size ranging between 132 to 175 µm. From the experimental observations, it is evident that the *ES* can achieve high removal rate (>95%), indeed become a promising eco-friendly biosorptive material for MB dye removal.

Keywords: *Biosorbent, Euchema spinosum, Methylene Blue, decolourization, Response Surface Methodology, Artificial Neural Network*

1. Introduction

The extensive use of synthetic-based dye in various applications in modern living today has notably led to severe wastewater problem[1]. Over 700,000 tons of commercial dyes are widely employed in textile, food, pharmaceutical, printing, paper, paint, leather industries [2]. Approximately 15% of the estimated usage of dye appear in wastewater effluent [3]. At trace level, the dye may cause serious environmental pollution. Dye and their degradation product may produce mutagenic, genotoxic, carcinogenic and teratogenic effect onto the receptor water bodies [4].Their complex structures form a stable molecular that is difficult to degrade due to the presence of aromatic rings and azo functional group (N=N) [2]. Treatment process from simple to sophisticated methods has been employed to treat the dye contained wastewater, such as coagulation-flocculation, precipitation, ion exchange, filtration, ozonation and advanced oxidation [5]–[9] . However, more often than not, they are either ineffective or highly expensive [10].

Euchema Spinosum (also known as *Euchema denticulatum*) is red alga that is massively grown in Sabah, Malaysia. Biosorption capacity of red algae is attributed mainly by the presence of sulfated polysaccharides in its cell walls [20], [21]. The previous study on *ES* as biosorbent is based on one factor at time effect (OFAT) which is time consuming, tedious and involved a large sample size leading to high cost of experimentation. Furthermore, through the employment of OFAT, the simultaneous assessment of the effect of several parameters is not possible, that in turn, may lead to inaccurate prediction of optimisation. Therefore, multivariate statistical technique, as well as machine learning algorithm, has been employed to mitigate the limitation of classical analysis.

RSM is a practical method for studying the effect of multiple parameters, determining the significant parameters and analysing the possible interactions that may influence the biosorption process [22], [23]. RSM considerably reduces the number of experimental runs, provide information on the interaction between parameters and determine the optimum operational conditions yielding the highest removal efficiency [24]. In this study, the Central Composite Design (CCD) is employed to determine the optimum process

Copyright © 2018 Authors. This is an open access article distributed under the Creative Commons Attribution License, which permits unrestricted use, distribution, and reproduction in any medium, provided the original work is properly cited.

variables. CCD has better predictive capabilities based on linear and quadratic interaction effect among significant factors affecting the process [25]. A number of study has utilised CCD for adsorption process such as biosorption of methylene blue (MB) onto low-cost Lemna major biomass [26], adsorption of sunset yellow (SY), malachite green (MG), methylene blue (MB) onto Cu@ Mn-ZnS-NPs-AC[27], removal of eosin Y (EY), methylene blue (MB) and phenol red (PR), by Cu(OH)2-NP-AC [28] and biosorption of real textile effluent onto deoiled Argemone Mexicana seeds (A. Mexicana) [23]. A study on the removal of copper(II) ions waste flax meal [29], further suggests that CCD has the capability to provide reasonably accurate predictions.

McCulloh and Pitts (1943) initiated the artificial neural network (ANN) model based on how neurons behave in the nervous system. Today, ANN is a prevalent method of analysis due to its effectiveness in many scientific fields [30]–[40]. The input along with its weights and threshold value will determine the output of the model. A biosorption system is inherently a non-linear system in nature [41]. It is evident from the literature that ANN has successfully been used for predictive modelling in the area of biosorption. ANN modelling was employed to predict the adsorption capacity of Acid Black 172 metal-complex dye (AB) and Congo Red (CR) using nonviable Penicillium YW 01 biomass [42]. The removal efficiency prediction model of Lanaset Red (LR) G on walnut husk (WH) was developed by means of ANN [43]. In a recent study, it was reported that ANN modelling was used to predict the removal of non-toxic dye by Graphene oxide (GO) nanoplatelets and an R of 0.96452 was reported with network topology of 3-10-1 [44].

ES as dye biosorbent has never been reported in term of pretreatment effect, optimization and reusability but batch biosorption using OFAT method has been documented previously[45]. Therefore, the main motivation behind the study is to expands the body of knowledge of *ES* on the capability of the aforesaid biosorbent to (1) undergo pretreatment; (2) the determination of the optimal experimental condition for maximum removal efficiency using contemporary multivariate models namely Response Surface Methodology (RSM) and Artificial Neural Networks (ANN), and; (3) its ability to be reused with regards to its economical viability.

2. Experiment Section

2.1. Material and Equipment

A stock solution of Methylene Blue (MB) dye was initially prepared by dissolving a weighed quantity of $C_{16}H_{18}C_lN_3S\cdot_2H_2O$ in deionized water. By conducting a serial dilution, the working solutions were prepared to the desired concentration of 100-500 mg/L. All chemicals were used as received without further purification.

Red alga of ES was collected from Kunak, Sabah (Fig. 1). The ES was washed three times thoroughly with deionised water to remove sand, salts and epiphytes. The alga was dried at 60 ºC for 24 h in a drying oven,then, was ground and sieved in order to attain the size range of 0.7 to 1.5 mm that adheres to the Standard ISO3310-1:2000 (British Standard) sieves. The prepared biosorbent are then kept in a zip-locked bag until further process is carried out.



Fig. 1: Fresh macroalga of Euchema Spinosum (ES)

2.2. Experimental Procedure

Batch biosorption experiments were carried out for MB dye removal using ES biosorbent for RSM design experiment. All 20 experimental runs were carried out in 25 mL vials containing 25 mL of MB dye solution with the initial concentration ranged between 100-500 mg/L with varying dosage (0.3-1.1g/L), pH (2-12) and fixed equilibrium contact time (60 min). The vials were placed into a shaker and held at a constant speed of 130 rpm for 1h. After equilibrium is reached, the solutions were centrifuged at 4000 rpm for 60 sec. The final concentration of the MB dye in the supernatant solution was analyzed using the UV-Vis spectrophotometric. All measurements were performed in triplicate. The removal efficiency (y,%) and the amount of MB dye adsorbed (qe, mg/g) were calculated based on equation (1)and (2) :

$$\text{MB dye removal, y(\%)} : \frac{C_i - C_e}{C_i} \times 100 \quad (1)$$

$$\text{MB dye biosorption capacity, qe (mg/g)} : \frac{(C_i - C_e)\forall}{M} \quad (2)$$

Where y is percentage removal, qe is the amount of MB dye sorbed per gram of biosorbent at equilibrium (mg/g), Ci and Ce are the initial and equilibrium MB concentration in the solution (mg/L), respectively, ∀ is the MB solution volume (L) and m is the biosorbent mass (g).

2.3. Analytical Equipment

The initial and residual concentration of MB dye (HmBG) for the biosorption-desorption process was estimated using the UV-Vis spectrophotometric (UV-Vis spectrophotometer, DR5000, Arachem) at 650nm (λmax). pH of the dye solution was maintained by adding NaOH or/and HCl (Merck, Germany) and determined with a pH meter (SevenEasypH, Mettler-Toledo AG, Schwerzenbach, Switzerland). Deionized water was used for all experiments (Puris-Expe CB Water System, 18.2MΩ.cm resistivity). A Memmert oven (model UFB500, Germany) and furnace (Carbolite furnace, model ELF 11/23, England) was used for the drying purpose. The shaker (Excella E1 Platform shaker, New Jersey, USA) was used to provide uniform mixing between biosorbent and sorbate, while centrifuge (Centrifuge, model 2420, Tokyo, Japan) were used to accelerate the phase separation. Prior to the determination of the optimal conditions, the ES sample were examined for functional group, morphologies characteristic and thermal analysis using Fourier Transform Infrared Spectrophotometer (FTIR, spectrum 100 Perkin-Elmer), Scanning Electron Microscopy with Energy Dispersive X-Ray Analysis (SEM-EDX, TM3030plus, Hitachi, Japan) and Thermo Gravimetric Analysis (TGA, Mettle Toledo), respectively.

2.4. Response Surface Methodology (RSM)

In this study, the central composite design (CCD) was applied as a design tool for dye biosorption using ES biomass. The parameters whose simultaneous effects on removal efficiency are employed and further modelled using CCD. In CCD, the numeric factors will be varied over 5 levels; axial points (+/-alpha), factorial points (+/-1) and centre point. Centre points give assistant to the calculation of pure error whilst the axial points allow the design to be rotatable. The correlation between variables and response is expressed using second-order polynomial quadratic model, given as in equation (3).

$$y_{MB\ dye} = \beta_o + \sum_{i=1}^{3} \beta_i x_i + \sum_{i=1}^{3} \sum_{j=1}^{3} \beta_{ij} x_i x_j + \sum_{i=1}^{3} \beta_{ii} x_i^2 \quad (3)$$

where y is the response (% predicted removal); x is the independent parameter (contact time, pH, dosage), i and j represent a number of factors, βo is the constant coefficient, βi are linear coefficients, βij are interaction coefficients, and βii is quadratic coefficients.
The parameter settings used for running RSM model is presented in Table 2.1. The data were analysed using Stat-Ease (Design Expert 7.0.0, Minneapolis) and the coefficients were interpreted using p- and F-values. The F-value is the ratio of mean square regression and means square residual, which serves as an excellent indicator to distinguish and discriminate among different parameters in terms of their significant contribution on signal [60]. The accuracy of model fitting is evaluated by means of analysis of variance (ANOVA) based on the coefficient of determination (R^2), adjusted determination coefficient (adj-R^2), predicted determination coefficient (pred-R^2), coefficient of variation (CV) and adequate precision (AP). The optimisation was calculated based on the regression analysis and 3D response surface plot.

2.5. Artificial Neural Network

Prediction of dye removal in this investigation is modelled using the multilayer Feedforward Neural Network Architecture specifically multilayer perceptron (MLP) network. MLP is made up of one or more hidden neuron layers where computation takes place. The weighted output from the first hidden layer is used as input for the output neurons or for the subsequent hidden layers. The network topology of 3-7-1 utilised in this study is depicted in Fig. 2 which shows that there are three input nodes, seven neurons in the single hidden layer and one neuron in the output layer. This kind of topology is known as multi-input single-output (MISO). Multi-input-multi-output (MIMO) is used when there is more than one output to be analysed with multi-input. Single-input-single-output (SISO) is used when there is only one input and one output to be analysed.

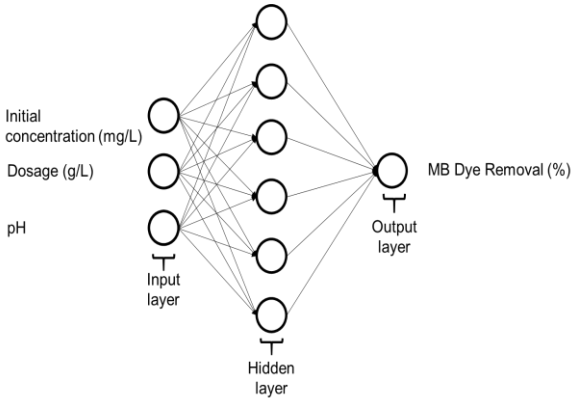


Fig. 2: ANN network topology

The implementation of ANN comprises of three main stages viz. parameter selection, training and testing. The input-output data is often processed by normalising it within a certain range, nonetheless, it is worth noting that there are studies that take the data as is without performing any form of scaling. The data is then randomly partitioned with respect to training, testing and/or validation, respectively. Amongst the key parameters that are specified prior to any ANN investigation are the selection of the input and output parameters, the number of hidden layers, the number of neurons in the hidden layers, the activation function, as well as the training (learning) algorithms.

The 3 main phases of ANN are viz. parameter selection, training and testing. The input and output data can be taken as it is or it can be normalised. The data will be randomly segregated with respect to training, testing and/or validation, respectively. In this study, tangent sigmoid (tansig) transfer function is utilised in the hidden layer whereas the linear (purelin) transfer function is used in the output layer. The Levenberg- Marquardt training algorithm is utilised to train the dataset. By varying the number of neurons from one to ten, seven hidden neurons were deemed optimal to provide desirable results upon carrying out a sensitivity test. Initial concentration, dosage and pH were set as the input whereas MB dye removal percentage was set as the output. The 70:15:15 ratio is employed for the training, testing and validation of the models developed on the prepared dataset. The prediction model is validated and verified using mean-square error (MSE) and regression analysis (R^2). Design parameters used for ANN in this study are summarised in

Table 1. The study of ANN modeling was performed using MATLAB (Version R2017a) software.

Table 1: Parameter settings for RSM and ANN

RSM		ANN	
Parameters	Values	Parameters	Value
Design methodology	Central Composite	Learning rule	Levenberg-Marquardt
Design model	Quadratic	Number of input nodes	3
No of run	20	Number of output nodes	1
Input variables	3	Number of hidden neurons	7
Output Blocks	1 No blocks	Number of epochs Mu	12 0.001

3. Results and Discussion

3.1. Modelling of RSM

CCD was used to understand the influence and interaction between parameters, predict the different input parameters and further determine the optimal level of the process parameters. In the preliminary step of optimisation, the selected initial concentration (mg/L), dosage (g/L) and pH was taken. The biosorption process was considered under equilibrium condition with a contact time of 60 min at ambient temperature 27±3ºC [45]

3.1.1 Fitting Model and Analysis of Variance (ANOVA)

In this study, three independent variables were considered for the biosorption process namely; initial concentration (x_1: 200-400 mg/L), dosage (x_2: 0.5-0.9 g/L) and pH (x_3: pH 4.5-9.5) while the MB removal at equilibrium time is set as the response (y). By using CCD matrix of experimental condition, 20 runs were carried out (

$$= 95.08 - 8.29x_1 + 7.88x_2 - 0.68x_3 + 6.9x_1x_2 - 1.54x_1x_3 - 1.74x_2x_3 - 4.98x_1^2 - 4.56x_2^2 - 1.18x_3^2 \quad (4)$$

Table 3). The final CCD was second-order polynomial quadratic model and is given as in (4)

MB dye removal, $(y\%)$

The coefficient magnitude in the second-order polynomial quadratic equation(4) indicates the positive and negative effect of the factors to the response (% removal). In this regard, the positive term such as x_2, x_1x_2 denoted the favourable effect which depicted

the parameters will increase the removal efficiency with the increase of these parameters value. In contrast, the negative terms such as x_1, x_3, x_1x_3, x_2x_3, x_1^2, x_2^2 and x_3^2 demonstrate the unfavourable effect on the biosorption process. Therefore, the removal efficiency will be increased with the decrease of these parameters value. At confidence level of 95% ($p<0.05$), the linear term (x_1, x_2), interactive terms (x_1x_2, x_1x_3 ,x_2x_3) and square terms (x_1^2, x_2^2, x_3^2) showed significant effect on the response variable except for x_3 ($p< 0.0142$). Values of p-value greater than 0.1 indicate the model terms are not significant. It is evident, as tabulated in

Table 4, it can be shown that all model term used in this study is significant.

In order to ensure the statistical significance of above quadratic model, the model was tested using analysis of variance (ANOVA). **Table 4** represents the ANOVA results for MB biosorption onto *ES*. The model F-value (131.85) with low probability value ($p < 0.0001$) denotes that the model was significant, accurate and reliable. The goodness of fit for the models was examined for R^2, adj.-R^2, pred.-R^2, CV and AP. The value of R^2 should be at least 0.80 for the good fit of a model [46]. In this study, the R^2 was found to be 0.9916, indicate that over 99.16% of the experimental data was compatible with the data predicted by the model. The predicted R^2 (0.93) is in reasonable agreement with the adjusted R^2 (0.98). In addition, a lower CV (1.98%) demonstrate the deviations between experimental and predicted values were relatively low. A CV of not more than 10% can be considered as reasonable for a goodness of the model [47]. Therefore, the result potray that the experiment has better precision and reliable value. The AP is a measure of the signal to noise ratio in which value higher than 4 is desirable for the fitness of the model. The AP was obtained at 30.15 indicates the adequate model discrimination [48]. AP value greater than 4 is suggested for significant RSM modelling [12]. The model was also assessed for its suitability based on lack of fit. From the result, the higher F-test value (19.13) and low probability (P=0.0028) implies the lack of fit is significant with due to noise. This suggests that the RSM model is unable to provide a high prediction accuracy of the MB dye removal efficiency. A similar observation has also been reported by Hamid et al. (2016) [49] on the removal of Cu(II) from water matrix. In order to mitigate the aforesaid issue, an ANN model is developed.

3.1.2 Interactive Effect of Variables

The effect of parameters was deeply studied individually in the previous part of the study. However, less information can be derived from the relationship between parameters. Therefore, this section is dedicated to discuss the relationship between independent variables x_1 (initial concentration), x_2 (dosage) and x_3 (pH) on the removal efficiency (y%) of MB dye. 3D response surface plots and the corresponding contour plots for interaction between dosage-pH, initial concentration-pH and initial concentration-dosage are illustrated in **Fig. 3**(a)-(b), (c)- (d) and (e)-(f).

It can be seen in **Fig. 3**(a)- (b); the MB dye removal has increased from 83.6 to 94.44% with the increase of dosage (0.5 to 0.9g/L) which can be related to the higher number of active site for biosorption process. Further increase of dosage, however, shows a gradual decrease in removal efficiency, due to the saturated binding site. The effect of pH on removal rate is not favourable under the considered range of pH 5.75 to 8.25 at a lower dosage (0.5-0.7 gL). In the basic solution (pH> 8.25), an active functional group in ES biosorbent is less protonated, and the surface charge becomes negative by adsorbing OH- ions. Therefore, negatively charged surface sites on ES favoured the adsorption of the cationic MB dye molecule due to the electrostatic attraction. A similar agreement was reported on the adsorption of Acridine orange by zinc oxide/almond shell activated carbon composite [50].

As illustrated in **Fig. 3**(c)-(d), the increase in initial MB dye concentration (200 to 400 mg/L) has reduced the removal rate from 95.24% to 81.77%. It clearly depicts that the change in removal efficiency is not noticeable with the change of pH but the slight increased of removal rate was found merely at pH7. These results comply with studies carried out by previous work on various biosorbent, which have reported an optimum pH of 7 for maximum MB dye removal [51]–[53]

According to **Fig. 3**(e)-(f), the removal rate was decreased significantly from 92.95% to 68.57% with the increased in initial concentration (100 to 500 mg/L). This is possibly due to the lower concentration that increases the availability of vacant sites and in turn, increases the uptake of dye molecules onto ES biosorbent. Meanwhile, at a higher concentration with the same dosage, the same fixed number of biosorbent sites competes for more dye molecules, hence saturating it [23]. In addition, the increase of initial concentration would protonate the active sites in ES cell wall, hence reducing the repulsion strength between MB dye molecules and ES biosorbent thus leading to a decrement in the biosorption uptake and removal rate [24].

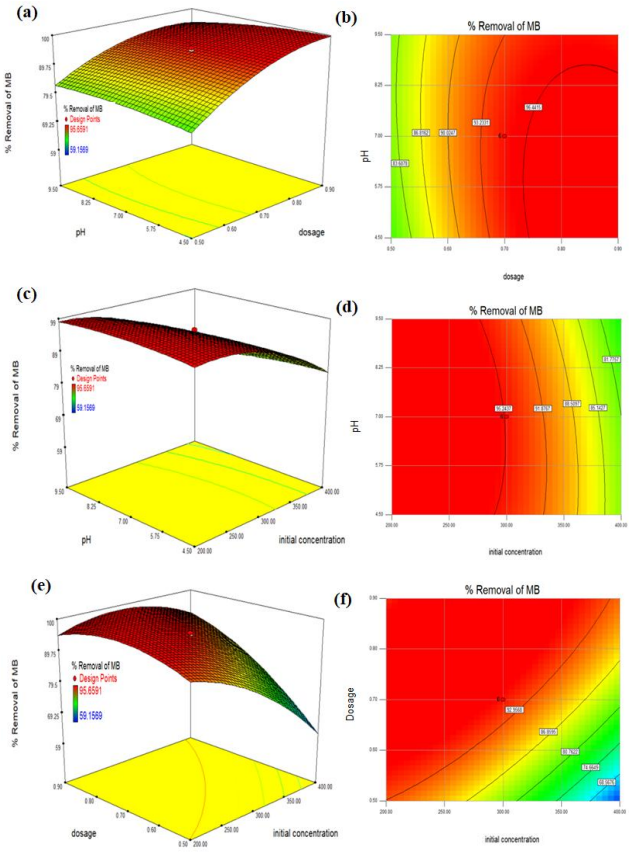


Fig. 3: 3D diagram and contour plot for MB dye removal efficiency as a function of; (a)-(b) dosage and pH ;(c)-(d) initial concentration and pH ;(e)-(f)initial concentration and dosage

3.2. Optimization of *ES* Biosorption

Process optimisation was achieved using a numerical node of the design expert software. This process involves specifying the target value for initial concentration to 300 mg/L, whilst keeping the rest (dosage and pH) within the range value. By determining the desirability score to 1.0, a maximum predicted MB removal of 95.9 % (qe= 398.09 mg/g) was obtained at optimised conditions set as follows: 300 mg/L of MB, biosorbent dosage of 0.72 g/L at pH6.9. The conduction of six replicates at specified optimum condition shows good agreement with predicted result. The obtained optimum conditions were validated by running similar experiments at the specified optimum condition, and the results were found to be 95.4% ± 0.4. This confirms the applicability of CCD in predicting the real behaviour of biosorption study.

SEM analysis was used to determine the porosity and particle shape of the biosorbent [54]. From the SEM images, it is apparent that the raw *ES* surface (**Fig. 4**a) has irregular shapes with cavities. However, after biosorption of the MB dye molecules onto the *ES* at optimal condition (Fig**. 4**b), it is observed that the formation of a considerable number of pores with varying diameter size ranging between 132-185µm (Error! Reference source not found.), indicating an effective biosorption of MB dye molecules onto the *ES* surface transpired.

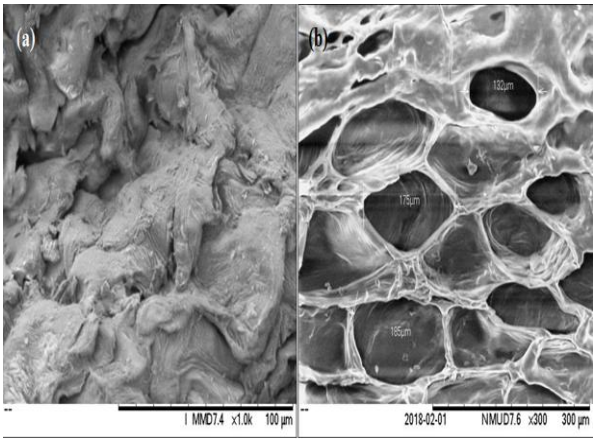


Fig. 4: SEM image of ES (a) before biosorption, (b) after biosorption at optimal condition of initial concentration 300 mg/L, pH6.9-7.1, dosage 0.72 g/L.

3.3. Modelling by ANN

In this study, the experimental data obtained from the RSM design were utilised. A total of 20 experiments from CCD was divided into three subsets comprising of training (14 data), validation (3 data) and testing (3 data), respectively. As previously mentioned, a sensitivity test by varying the number of neurons in the hidden layer from one to ten was carried out to obtain the optimum network topology. It was established from the sensitivity test that the optimum number of neurons in the hidden layer is seven as it provided the least MSE (< 0.3) and a high R^2 value of 0.99 (**Table 2**). **Fig. 5** depicts the correlation between the output (predicted values) and target (experimental values) for the training, testing and validation steps of the best network topology, i.e., 3-7-1.

Table 2: Comparison of 10 neurons in the hidden layer using a Lavenberg-Marquardt algorithm for the removal of MB dye using ANN model.

No of neuron	Train		Validate		Test	
	MSE	R^2	MSE	R^2	MSE	R^2
1	2.20	0.96	1.48	0.99	3.7	0.99
2	2.5	0.97	4.4	0.99	5.14	0.99
3	3.4	0.98	3.6	0.98	3.82	0.98
4	0.3	0.99	0.9	0.96	1.31	0.96
5	0.2	0.99	0.19	0.99	1.21	0.99
6	0.35	0.99	0.6	0.99	0.21	0.99
7	**0.17**	**0.99**	**0.28**	**0.99**	**0.20**	**0.99**
8	0.8	0.99	0.35	0.98	0.32	0.98
9	0.11	0.99	0.31	0.97	1.5	0.99
10	0.04	0.99	0.37	0.99	0.36	0.97

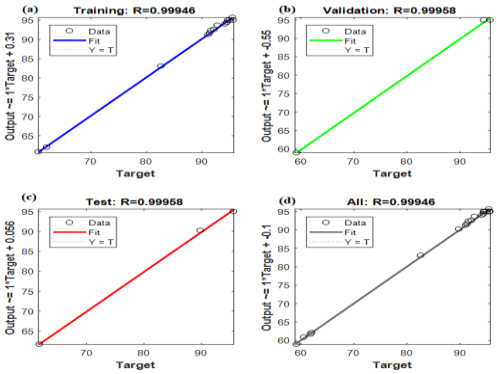


Fig. 5: The correlation between output and target of the ANN model (a) in training step, (b) in validation step, (c) in test step and (d) in overall. T is target values; Y is predicted output by model; and *R* correlation coefficient between the output of model and target values.

Table 3: Experimental data for CCD-RSM

Independent variables	unit	Symbol	Range and levels (coded)				
			-α	-1	0	+1	-α
Initial concentration	mg/L	x_1	100	200	300	400	500
Biosorbent dosage	g/L	x_2	0.3	0.5	0.7	0.9	1.1
pH		x_3	2	4.5	7	9.5	12
Run		x_1	x_2	x_3	qe(mg/g)	$\%y_e$	$\%y_{p,RSM}$
1		100	0.7	7	130.90	91.63	91.76
2		200	0.5	4.5	364.99	91.12	89.08
3		200	0.9	9.5	204.86	92.19	92.80
4		200	0.5	9.5	376.52	94.13	94.34
5		200	0.9	4.5	206.12	92.76	94.52
6		300	0.7	12	384.91	89.81	89.12
7		300	0.7	7	409.80	95.62	95.14
8		300	0.7	7	405.58	94.64	95.14
9		300	0.7	7	407.07	94.98	95.14
10		300	0.3	7	404.83	60.58	61.16
11		300	0.7	2	391.76	91.41	91.76
12		300	0.7	7	591.56	94.46	95.14
13		300	1.1	7	409.74	95.48	92.66
14		300	0.7	7	409.96	95.61	95.14
15		300	0.7	7	259.19	95.66	95.14
16		400	0.5	9.5	496.53	62.07	60.95
17		400	0.9	4.5	374.29	94.48	94.91
18		400	0.5	4.5	494.68	61.84	61.87
19		400	0.9	9.5	374.29	82.63	87.02
20		500	0.7	7	422.84	59.20	58.76

Table 4: ANOVA for MB dye removal

source	Sum of square	[a]Df	Mean square	F-value	p-value		status
model	3476.18	9	386.24	131.85	<0.0001		significant

x_1	1098.85	1	1098.85	375.12	<0.0001		significant
x_2	994.22	1	994.22	339.4	<0.0001		significant
x_3	7.45	1	7.45	2.54	0.1420		not significant
x_1x_2	381.18	1	381.18	130.13	<0.0001		significant
x_1x_3	19.06	1	19.06	6.51	0.0288		significant
x_2x_3	24.29	1	24.29	8.29	0.0164		significant
x_1^2	623.15	1	623.15	212.73	<0.0001		significant
x_2^2	522.21	1	522.21	178.27	<0.0001		significant
x_3^2	34.94	1	34.94	11.93	0.0062		significant
Residual	29.29	10	2.93				
Lack of fit	27.84	5	5.57	19.13	0.0028		significant
Pure error	1.46	5	0.29				
Cor total	3505.47	19					
Model statistic							
Response	Standard deviation (SD)	Mean values	Coefficient of variation (C-V%)	R^2	Adj-R^2	Pred-R^2	Adequate precision
%R MB	1.71	86.51	1.98	0.9916	0.9841	0.9356	30.150

[a] Degree of freedom

3.4. Statistical Comparison of RSM and ANN

The capability of RSM and ANN in predicting dye removal by ES were further evaluated statistically for fitness parameters such as coefficient of determination (R^2), adjusted R^2 (adj-R^2), mean square error (MSE), root mean squared error (RMSE), mean absolute percentage error (MAPE) and average absolute relative error (AARE) are expressed in (5) to (8)[49], [55]

$$MSE = \frac{1}{n}\sum_{i=1}^{n}(y_p - y_e)^2 \quad (5)$$

$$RMSE = \sqrt{\frac{1}{n}\sum_{i=1}^{n}(y_p - y_e)^2} \quad (6)$$

$$MAPE = \frac{1}{n}\sum_{i=1}^{n}\left|\frac{y_p - y_e}{y_e}\right| X\,100 \quad (7)$$

$$AARE = \frac{1}{n}\sum_{i=1}^{n}\left|\frac{y_p - y_e}{y_e}\right| \quad (8)$$

where n is the number of experiments, yp is the predicted value, and ye is the experimental value.
The information on R^2 and adj-R^2 is useful as it indicates how well the experimental data fit the model. In addition, adjusted R^2 penalise the additional independent variables which do not fit the model. A similar value between R^2 and adj-R^2 confirms the validity of the model. The lower values of MSE, RMSE, MAPE and AARE suggest that the model has low deviation.
The value of error parameters for both models is tabulated in
Table 6. The R^2 for both models (R^2_{RSM} = 0.9916 and R^2_{ANN} =0.9994) indicates that both models provided good quality predictions (**Fig. 6**). However, with a higher adj-R^2 of ANN (adj-R^2_{ANN}= 0.9992) in comparison to RSM (adj-R^2_{RSM} = 0.9841), it is apparent that the removal prediction made by ANN is more accurate. The error parameter for ANN (MSE=0.19, RMSE=0.4391, MAPE=0.087 and AARE=0.001) is demonstrated to be much lower than RSM (MSE=1.95, RMSE=1.395, MAPE=0.08 and AARE=0.001) further indicates that removal prediction by ANN is better than RSM with low error deviation.
For validation purposed, additional set of experimental data using 10 new trials which do not belong to the training data set was tested. The actual, predicted and residual value is tabulated in
Table 6. The R^2 and adj-R^2 for newly constructed ANN and RSM model indicating the removal prediction for validation data is better fit with ANN model (R^2=0.8911) than RSM (R^2= 0.7124)(**Fig. 7**). Moreover, the lower values of MSE, RMSE, MAPE and AARE further suggest that the ANN model has a better prediction than the RSM model. Model performance and comparison between dataset and validation data for both model is shown in
Table 6. It is evident that the ANN modelling technique is far more superior in comparison to the RSM modelling in predicting the removal efficiency

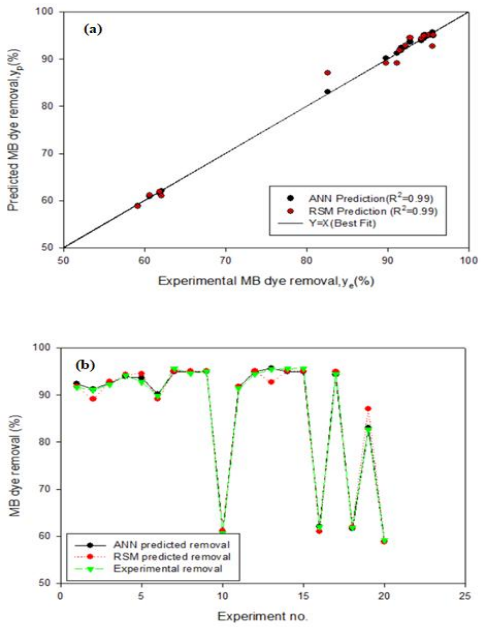


Fig. 6: Comparison of (a) Regression graph for prediction using ANN and RSM models and, (b) experimental removal to predicted value achieved by the RSM and ANN models

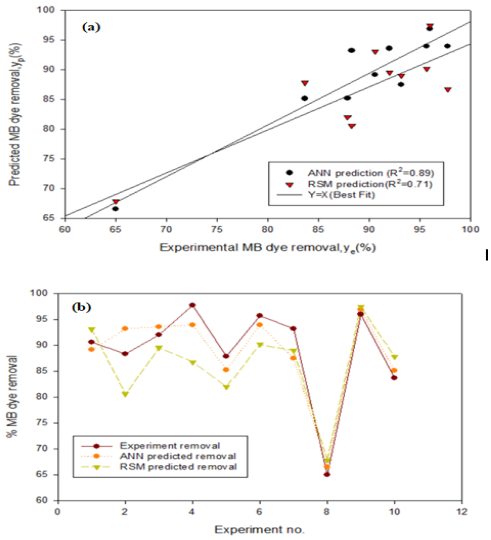


Fig. 7: Comparison of (a) Regression graph for prediction using ANN and RSM models and, (b) experimental removal to predicted value achieved by the RSM and ANN models; for validation data

Table 5: Validation data

No.of run	x_1	x_2	x_3	Biosorption capacity	MB removal (%)	RSM		ANN	
				qe	ye	y_{pRSM}	Residual	y_{pANN}	Residual
1	100	0.5	7	181.21	90.61	93.13	-2.52	89.17	1.44
2	140	1	7	83.61	88.30	80.62	7.68	93.24	-4.95
3	150	1	7	68.04	92.03	89.56	2.47	93.61	-1.58
4	160	1	7	51.62	97.77	86.78	10.99	93.96	0.81
5	200	0.4	4.5	439.37	87.87	82.03	5.84	85.26	2.62
6	200	1	4.5	199.43	95.67	90.19	5.48	93.97	1.70
7	200	0.4	9.5	465.83	93.17	89.03	4.14	87.53	5.64
8	300	0.4	7	516.11	65.00	67.85	-2.85	66.55	-1.55
9	400	1	4.5	384.01	96.00	97.48	-1.47	96.89	-0.89
10	400	1	9.5	311.38	83.67	87.85	-4.18	85.15	-1.48

Table 6: Model performance and comparison

Statistical evaluation parameters	Models			
	RSM		ANN	
	CCD (20 dataset)	Validation (10 dataset)	CCD (20 dataset)	Validation (10 dataset)
R^2	0.9916	0.7124	0.9994	0.8911
Adj-R^2	0.9841	0.6766	0.9992	0.8734
MSE	1.95	30.1180	0.19	9.0492
RMSE	1.395	5.4881	0.4391	3.03887
MAPE	0.08	2.5738	0.087	0.3887
AARE	0.001	0.0257	0.001	0.0039

4. Conclusion

The effect of initial concentration, dosage and pH on MB dye removal using untreated *ES* were investigated by means of RSM and ANN method. The removal prediction using RSM revealed that the effect of independent variables in the biosorption process in which, dosage and initial concentration gives positive effect onto the process to yield high removal efficiency. At optimal condition, the extreme morphology changes on the surface of *ES* was observed, with the formation of a considerable number of pores.. The feed-forward multilayered perceptron ANN trained using back-propagation algorithms was used for the prediction of MB dye removal. Both RSM and ANN models showed a good predictive capabilities (R^2 values > 0.99). Through statistical evaluation, the predicted response for both models was compared with the actual experimental values. The adjusted R^2 (adj-R^2), mean square error (MSE), root mean squared error (RMSE), mean absolute percentage error (MAPE) and average absolute relative error (AARE) performance metrics were used together to compare the performance of RSM and ANN. The results revealed that prediction of RSM (adj-R^2= 0.9841, MSE=1.95, RMSE=1.395, MAPE=0.08 and AARE=0.001) has greater deviation in comparison to the prediction made using ANN modelling (adj-R^2=0.9916, MSE=0.19, RMSE=0.4391, MAPE=0.087 and AARE=0.001). To further validate the predictive capability of both models, the validation study was carried out using additional data. It was shown statistically that the ANN developed model is more superior than the RSM model in fitting the additional data, suggesting a higher fidelity model was developed via ANN. As a concluding remark, it is evident from the results obtained from the present study that *ES* is a potentially effective and green biosorbent dye removal owing to its excellent biosorption at extreme dye concentration and pH.

References

[1] B. H. Hameed, "Removal of cationic dye from aqueous solution using jackfruit peel as non-conventional low-cost adsorbent," *J. Hazard. Mater.*, vol. 162, no. 1, pp. 344–350, 2009.

[2] I. M. Reck, R. M. Paixão, R. Bergamasco, M. F. Vieira, and A. M. S. Vieira, "Removal of tartrazine from aqueous solutions using adsorbents based on activated carbon and Moringa oleifera seeds," *J. Clean. Prod.*, vol. 171, pp. 85–97, 2018.

[3] W. A. Khanday, F. Marrakchi, M. Asif, and B. H. Hameed, "Mesoporous zeolite–activated carbon composite from oil palm ash as an effective adsorbent for methylene blue," *J. Taiwan Inst. Chem. Eng.*, vol. 70, pp. 32–41, 2017.

[4] B. Royer *et al.*, "Applications of Brazilian pine-fruit shell in natural and carbonized forms as adsorbents to removal of methylene blue

from aqueous solutions-Kinetic and equilibrium study," *J. Hazard. Mater.*, vol. 164, no. 2–3, pp. 1213–1222, 2009.
[5] C. R. Holkar, A. J. Jadhav, D. V. Pinjari, N. M. Mahamuni, and A. B. Pandit, "A critical review on textile wastewater treatments: Possible approaches," *J. Environ. Manage.*, vol. 182, pp. 351–366, 2016.
[6] V. K. Gupta and Suhas, "Application of low-cost adsorbents for dye removal - A review," *J. Environ. Manage.*, vol. 90, no. 8, pp. 2313–2342, 2009.
[7] C. D. Raman and S. Kanmani, "Textile dye degradation using nano zero valent iron: A review," *J. Environ. Manage.*, vol. 177, pp. 341–355, 2016.
[8] A. K. Verma, R. R. Dash, and P. Bhunia, "A review on chemical coagulation / fl occulation technologies for removal of colour from textile wastewaters," *J. Environ. Manage.*, vol. 93, no. 1, pp. 154–168, 2012.
[9] N. Daneshvar, A. R. Khataee, and N. Djafarzadeh, "The use of artificial neural networks (ANN) for modeling of decolorization of textile dye solution containing C. I. Basic Yellow 28 by electrocoagulation process," *J. Hazard. Mater.*, 2006.
[10] N. Djebri, M. Boutahala, N.-E. Chelali, N. Boukhalfa, and L. Zeroual, "Enhanced removal of cationic dye by calcium alginate/organobentonite beads: Modeling, kinetics, equilibriums, thermodynamic and reusability studies," *Int. J. Biol. Macromol.*, vol. 92, pp. 1277–1287, 2016.
[11] I. Ali, M. Asim, and T. A. Khan, "Low cost adsorbents for the removal of organic pollutants from wastewater," *J. Environ. Manage.*, vol. 113, pp. 170–183, 2012.
[12] A. K. Nayak and A. Pal, "Green and efficient biosorptive removal of methylene blue by Abelmoschus esculentus seed: Process optimization and multi-variate modeling," *J. Environ. Manage.*, vol. 200, pp. 145–159, 2017.
[13] M. M. Areco, S. Hanela, J. Duran, and M. dos Santos Afonso, "Biosorption of Cu(II), Zn(II), Cd(II) and Pb(II) by dead biomasses of green alga Ulva lactuca and the development of a sustainable matrix for adsorption implementation," *J. Hazard. Mater.*, vol. 213–214, pp. 123–132, 2012.
[14] K. S. Hameed, P. Muthirulan, and M. M. Sundaram, "Adsorption of chromotrope dye onto activated carbons obtained from the seeds of various plants : Equilibrium and kinetics studies," *Arab. J. Chem.*, vol. 10, pp. S2225–S2233, 2017.
[15] L. S. Oliveira, A. S. Franca, T. M. Alves, and S. D. F. Rocha, "Evaluation of untreated coffee husks as potential biosorbents for treatment of dye contaminated waters," *J. Hazard. Mater.*, vol. 155, no. 3, pp. 507–512, 2008.
[16] N. Nasuha, B. H. Hameed, and A. T. M. Din, "Rejected tea as a potential low-cost adsorbent for the removal of methylene blue," *J. Hazard. Mater.*, vol. 175, no. 1–3, pp. 126–132, 2010.
[17] A. A. Peláez-Cid, A. M. Herrera-González, M. Salazar-Villanueva, and A. Bautista-Hernández, "Elimination of textile dyes using activated carbons prepared from vegetable residues and their characterization," *J. Environ. Manage.*, vol. 181, pp. 269–278, 2016.
[18] T. Ahmad and M. Danish, "Prospects of banana waste utilization in wastewater treatment: A review," *J. Environ. Manage.*, vol. 206, pp. 330–348, 2018.
[19] E. Daneshvar, A. Vazirzadeh, A. Niazi, M. Kousha, M. Naushad, and A. Bhatnagar, "Desorption of Methylene blue dye from brown macroalga: Effects of operating parameters, isotherm study and kinetic modeling," *J. Clean. Prod.*, vol. 152, pp. 443–453, 2017.
[20] C. E. Flores-Chaparro, L. F. Chazaro Ruiz, M. C. Alfaro de la Torre, M. A. Huerta-Diaz, and J. R. Rangel-Mendez, "Biosorption removal of benzene and toluene by three dried macroalgae at different ionic strength and temperatures: Algae biochemical composition and kinetics," *J. Environ. Manage.*, vol. 193, pp. 126–135, 2017.
[21] J. He and J. P. Chen, "A comprehensive review on biosorption of heavy metals by algal biomass: Materials, performances, chemistry, and modeling simulation tools," *Bioresour. Technol.*, vol. 160, pp. 67–78, 2014.
[22] D. Navamani Kartic, B. C. H. Aditya Narayana, and M. Arivazhagan, "Removal of high concentration of sulfate from pigment industry effluent by chemical precipitation using barium chloride: RSM and ANN modeling approach," *J. Environ. Manage.*, vol. 206, pp. 69–76, 2018.
[23] S. Khamparia and D. Jaspal, "Study of decolorisation of binary dye mixture by response surface methodology," *J. Environ. Manage.*, vol. 201, pp. 316–326, 2017.
[24] M. M. Momeni, D. Kahforoushan, F. Abbasi, and S. Ghanbarian, "Using Chitosan/CHPATC as coagulant to remove color and turbidity of industrial wastewater: Optimization through RSM design," *J. Environ. Manage.*, vol. 211, pp. 347–355, 2018.
[25] A. Witek-Krowiak, K. Chojnacka, D. Podstawczyk, A. Dawiec, and K. Pokomeda, "Application of response surface methodology and artificial neural network methods in modelling and optimization of biosorption process," *Bioresour. Technol.*, 2014.
[26] B. Sadhukhan, N. K. Mondal, and S. Chattoraj, "Optimisation using central composite design (CCD) and the desirability function for sorption of methylene blue from aqueous solution onto Lemna major," *Karbala Int. J. Mod. Sci.*, vol. 2, no. Ccd, pp. 145–155, 2016.
[27] M. Dastkhoon, M. Ghaedi, A. Asfaram, A. Goudarzi, S. M. Mohammadi, and S. Wang, "Improved adsorption performance of nanostructured composite by ultrasonic wave: Optimization through response surface methodology, isotherm and kinetic studies," *Ultrason. Sonochem.*, vol. 37, pp. 94–105, 2017.
[28] S. Dashamiri, M. Ghaedi, A. Asfaram, F. Zare, and S. Wang, "Multi-response optimization of ultrasound assisted competitive adsorption of dyes onto Cu (OH)2-nanoparticle loaded activated carbon: Central composite design," *Ultrason. Sonochem.*, vol. 34, pp. 343–353, 2017.
[29] D. Podstawczyk, A. Witek-Krowiak, A. Dawiec, and A. Bhatnagar, "Biosorption of copper(II) ions by flax meal: Empirical modeling and process optimization by response surface methodology (RSM) and artificial neural network (ANN) simulation," *Ecol. Eng.*, vol. 83, pp. 364–379, 2015.
[30] K. Hamad, M. Ali Khalil, and A. Shanableh, "Modeling roadway traffic noise in a hot climate using artificial neural networks," *Transp. Res. Part D Transp. Environ.*, vol. 53, pp. 161–177, 2017.
[31] M. Z. Božnar, B. Grašič, A. P. de Oliveira, J. Soares, and P. Mlakar, "Spatially transferable regional model for half-hourly values of diffuse solar radiation for general sky conditions based on perceptron artificial neural networks," *Renew. Energy*, vol. 103, pp. 794–810, 2017.
[32] G. Binetti *et al.*, "Cultivar classification of Apulian olive oils: Use of artificial neural networks for comparing NMR, NIR and merceological data," *Food Chem.*, vol. 219, pp. 131–138, 2017.
[33] H. Shabanpour, S. Yousefi, and R. F. Saen, "Forecasting efficiency of green suppliers by dynamic data envelopment analysis and artificial neural networks," *J. Clean. Prod.*, vol. 142, pp. 1098–1107, 2017.
[34] S. Raith *et al.*, "Artificial Neural Networks as a powerful numerical tool to classify specific features of a tooth based on 3D scan data," *Comput. Biol. Med.*, vol. 80, pp. 65–76, 2017.
[35] E. H. Shiguemori, J. D. S. Da Silva, and H. F. De Campos Velho, "Estimation of initial condition in heat conduction by neural network," *Inverse Probl. Sci. Eng.*, vol. 12, no. 3, pp. 317–328, 2004.
[36] E. P. Carden and P. Fanning, "Vibration based condition monitoring: A review," *Struct. Heal. Monit.*, vol. 3, no. 4, pp. 355–377, 2004.
[37] K. Worden and J. M. Dulieu-Barton, "An Overview of Intelligent Fault Detection in Systems and Structures," *Struct. Heal. Monit.*, vol. 3, no. 1, pp. 85–98, Mar. 2004.
[38] M. S. Hossain, Z. C. Ong, Z. Ismail, S. Noroozi, and S. Y. Khoo, "Artificial neural networks for vibration based inverse parametric identifications: A review," *Appl. Soft Comput.*, vol. 52, pp. 203–219, 2017.
[39] K. Yetilmezsoy and S. Demirel, "Artificial neural network (ANN) approach for modeling of Pb(II) adsorption from aqueous solution by Antep pistachio (Pistacia Vera L.) shells," *J. Hazard. Mater.*, 2008.
[40] R. M. Aghav, S. Kumar, and S. N. Mukherjee, "Artificial neural network modeling in competitive adsorption of phenol and resorcinol from water environment using some carbonaceous adsorbents," *J. Hazard. Mater.*, 2011.
[41] N. G. Turan, B. Mesci, and O. Ozgonenel, "Artificial neural network (ANN) approach for modeling Zn(II) adsorption from leachate using a new biosorbent," *Chem. Eng. J.*, 2011.
[42] Y. Yang *et al.*, "Biosorption of Acid Black 172 and Congo Red from aqueous solution by nonviable Penicillium YW 01: Kinetic study, equilibrium isotherm and artificial neural network modeling," *Bioresour. Technol.*, 2011.
[43] A. ??elekli, S. S. Birecikligil, F. Geyik, and H. Bozkurt, "Prediction of removal efficiency of Lanaset Red G on walnut husk using artificial neural network model," *Bioresour. Technol.*, 2012.

[44] P. Banerjee, S. Sau, P. Das, and A. Mukhopadhayay, "Optimization and modelling of synthetic azo dye wastewater treat- ment using Graphene oxide nanoplatelets: Characterization toxicity evaluation and optimization using Artificial Neural Network," *Ecotoxicol. Environ. Saf.*, vol. 119, pp. 47–57, 2015.
[45] N. Mokhtar, E. A. Aziz, A. Aris, W. F. W. Ishak, and N. S. Mohd Ali, "Biosorption of azo-dye using marine macro-alga of Euchema Spinosum," *J. Environ. Chem. Eng.*, vol. 5, no. 6, pp. 5721–5731, 2017.
[46] P. S. Ardekani, H. Karimi, M. Ghaedi, A. Asfaram, and M. K. Purkait, "Ultrasonic assisted removal of methylene blue on ultrasonically synthesized zinc hydroxide nanoparticles on activated carbon prepared from wood of cherry tree: Experimental design methodology and artificial neural network," *J. Mol. Liq.*, vol. 229, pp. 114–124, 2017.
[47] E. Inam, U. J. Etim, E. G. Akpabio, and S. A. Umoren, "Process optimization for the application of carbon from plantain peels in dye abstraction," *Integr. Med. Res.*, vol. 11, no. 1, pp. 173–185, 2017.
[48] A. R. Bagheri, M. Ghaedi, A. Asfaram, A. A. Bazrafshan, and R. Jannesar, "Comparative study on ultrasonic assisted adsorption of dyes from single system onto Fe3O4 magnetite nanoparticles loaded on activated carbon: Experimental design methodology," *Ultrason. Sonochem.*, vol. 34, pp. 294–304, 2017.
[49] H. A. Hamid, Y. Jenidi, W. Thielemans, C. Somerfield, and R. L. Gomes, "Predicting the capability of carboxylated cellulose nanowhiskers for the remediation of copper from water using response surface methodology (RSM) and artificial neural network (ANN) models," *Ind. Crop. Prod.*, vol. 93, pp. 108–120, 2016.
[50] M. Zbair, Z. Anfar, H. Ait Ahsaine, N. El Alem, and M. Ezahri, "Acridine orange adsorption by zinc oxide/almond shell activated carbon composite: Operational factors, mechanism and performance optimization using central composite design and surface modeling," *J. Environ. Manage.*, vol. 206, pp. 383–397, 2018.
[51] S. Zhao and T. Zhou, "Bioresource Technology Biosorption of methylene blue from wastewater by an extraction residue of Salvia miltiorrhiza Bge," *Bioresour. Technol.*, vol. 219, pp. 330–337, 2016.
[52] M. Ghaedi, N. Zeinali, A. M. Ghaedi, M. Teimuori, and J. Tashkhourian, "Artificial neural network-genetic algorithm based optimization for the adsorption of methylene blue and brilliant green from aqueous solution by graphite oxide nanoparticle," *Spectrochim. Acta - Part A Mol. Biomol. Spectrosc.*, 2014.
[53] D. Mitrogiannis, G. Markou, A. Çelekli, and H. Bozkurt, "Biosorption of methylene blue onto Arthrospira platensis biomass: Kinetic, equilibrium and thermodynamic studies," *J. Environ. Chem. Eng.*, vol. 3, no. 2, pp. 670–680, 2015.
[54] N. M. Mahmoodi, M. Arami, H. Bahrami, and S. Khorramfar, "Novel biosorbent (Canola hull): Surface characterization and dye removal ability at different cationic dye concentrations," *Desalination*, vol. 264, no. 1–2, pp. 134–142, 2010.
[55] S. Mandal, S. S. Mahapatra, M. K. Sahu, and R. K. Patel, "Artificial neural network modelling of As(III) removal from water by novel hybrid material," *Process Saf. Environ. Prot.*, vol. 93, no. November 2013, pp. 249–264, 2015.